Computers & Geosciences 49 (2012) 278–289

Contents lists available at SciVerse ScienceDirect

Computers & Geosciences

journal homepage: www.elsevier.com/locate/cageo

REGCONT: A Matlab based program for stable downward continuation of geophysical potential fields using Tikhonov regularization

R. Pašteka[a,*], R. Karcol[b], D. Kušnirák[a], A. Mojzeš[a]

[a] Department of applied and environmental geophysics, Comenius University, Mlynská dol., 842 15 Bratislava, Slovak Republic
[b] Geophysical Institute, Slovak Academy of Sciences, Dúbravská cesta 9, 845 28 Bratislava, Slovak Republic

ARTICLE INFO

Article history:
Received 2 January 2012
Received in revised form
9 June 2012
Accepted 11 June 2012
Available online 1 July 2012

Keywords:
Gravimetry
Magnetometry
Field continuation
Regularization
FFT
C-norm

ABSTRACT

Downward continuation of potential fields is a powerful, but very unstable tool used in the processing and interpretation of geophysical data sets. Treatment of the instability problem has been realized by various authors in different ways. The Tikhonov regularization approach is one of the most robust. It is based on a low-pass filter derivation in the Fourier spectral domain, by means of a minimization problem solution. We highlight the most important characteristics from its theoretical background and present its realization in the form of a Matlab-based program. The optimum regularization parameter value is selected as a local minimum of constructed L_p-norms functions—in the majority of cases, the *C*-norms give the best results. We demonstrate very good stabilizing properties of this method on several synthetic models and one real-world example from high-definition magnetometry. The main output of the proposed software solution is the estimation of the depth to source below the potential field measurement level.

© 2012 Elsevier Ltd. All rights reserved.

1. Introduction

Transformations of geophysical potential fields (mainly in gravimetry and magnetometry) play an important part during their processing and interpretation. Due to the harmonic property (fulfilling the Laplace equation) it is possible to realize the operation of analytical continuation of potential fields (upwards and downwards) in the source free domain. In the case, when we are continuing the data further from the sources, we are speaking about upward continuation, in the opposite direction (closer to the sources), we are dealing with downward continuation (we expect the sources below the measurement level, which is the common situation in applied geophysics). This description of the operation is independent of the orientation of the vertical coordinate axis, which can be different depending upon the application (either pointing downwards or upwards). In geophysical data processing, analytical continuation is used in various situations: e.g., to compare airborn and ground geophysical potential surveys data (measured on different height levels). In the interpretation of potential field data, upward continuation is used to enhance the regional components in the original data by suppressing near surface sources manifestation. Conversely continuation downwards is used to enhance the detection of shallower sources by extracting the local or residual anomalies (Fig. 1). Downward continuation is also often used to calculate the depth of the important shallowest sources. A great variety of mathematical treatments of the classical analytical continuation problem, either in space or spectral domain have been reported (Evjen, 1936; Tsuboi and Fuchida, 1937; Hughes, 1942; Bullard and Cooper, 1948; Peters, 1949 and many others; a good overview can be found in Roy, 2008). Strakhov in Mudretsova and Veselov (1990), p.328 defined two important aims of the downward continuation: (a) determination of the continued field itself and (b) estimation of the harmonic source-free space, where the continuation is possible (in other words: estimation of the depth of the shallowest sources).

From the point of view of potential theory, upward continuation is a stable transformation and it can be performed for any reasonable height level in the source free area (in the Fourier spectral domain, it is a low pass filter). A problem occurs in the case of downward continuation, as this is an unstable operation (e.g., Parker, 1977). It has been analytically derived from potential field theory by various authors (e.g., Baranov, 1975; p. 47–49), that we can only continue downwards an interconnected potential field function to the depth of its nearest source (its upper edge). However, in the case of the continuation of discrete potential field functions, approximated by series of orthogonal functions, we can numerically continue the potential field to arbitrary large depths (e.g., Jung, 1961, p. 240), even greater depths than that of the most shallow source. In the case of

* Corresponding author. Tel.: +4212 60296350.
E-mail address: pasteka@fns.uniba.sk (P. R.).

0098-3004/$ - see front matter © 2012 Elsevier Ltd. All rights reserved.
http://dx.doi.org/10.1016/j.cageo.2012.06.010

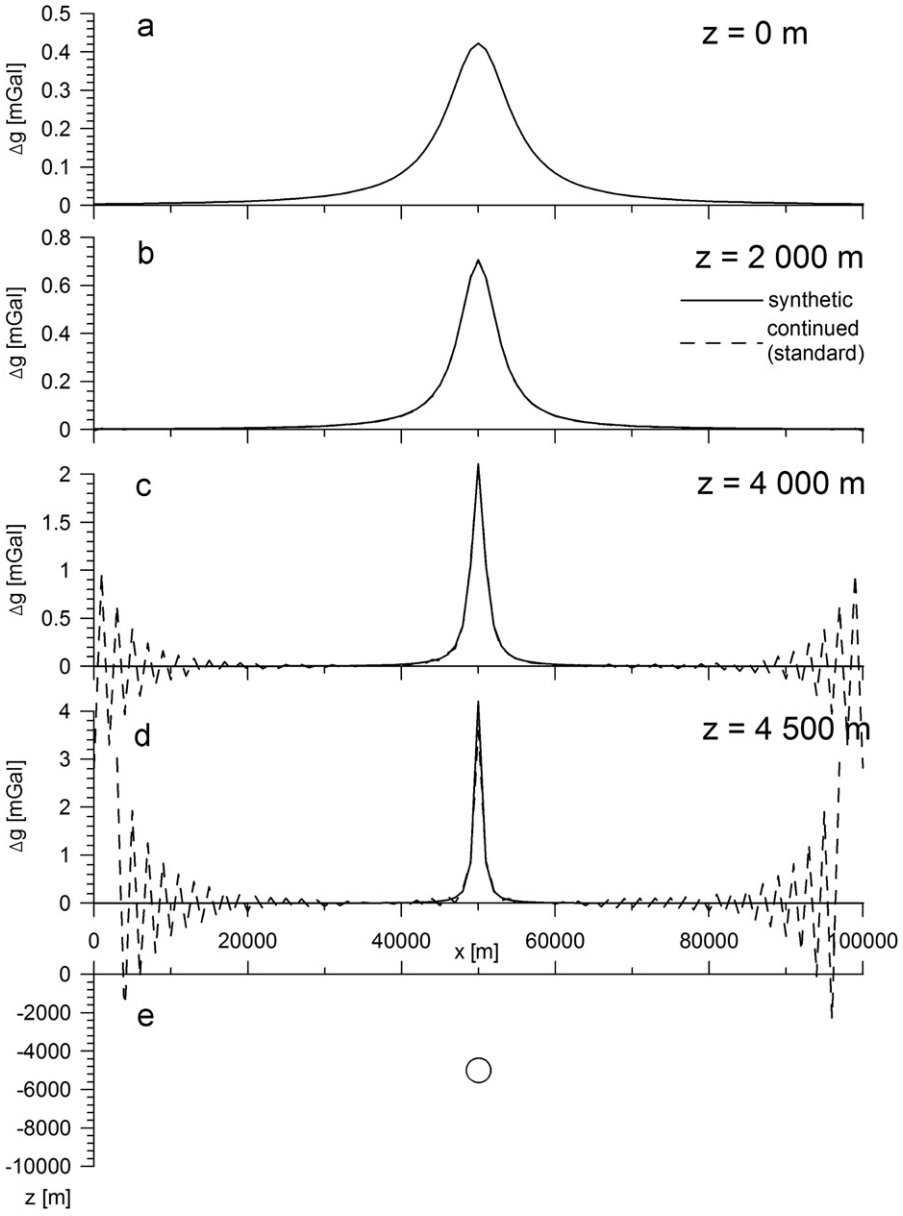

Fig. 1. Comparison of synthetic (full line) and downward continued (dashed line) gravitational field Δg by means of the standard approach in spectral domain for the case of a 2D horizontal cylinder in gravimetry (a) initial depth level $z=0$ m, (b) $z=2000$ m, (c) $z=4000$ m, (d) $z=4500$ m and (e) position of the cylinder in the xz-plane; parameters of the cylinder: centre depth=5000 m, radius=500 m, differential density=200 kg m^{-3}. 1 mGal=10^{-5} m s^{-2}.

isolated sources, this space of downward continuation is called by some authors the "quasi-harmonic region" (e.g., Fedi and Florio, 2011). Of course we must be aware of the fact that such a continued field is deformed (it does not correspond with the real field caused by the sources) and it is disturbed in the form of violent oscillations (Peters, 1949). In the Russian literature this is often described as the "disintegration" or "break-up of the field" (e.g., Mudretsova and Veselov, 1990, p.335). It is interesting to note that the disturbing oscillations have exactly the Nyquist wave-number of the continued discrete signal (e.g., Nabighian, 1974 or Berezkin, 1988, p. 68–75) due to the effect of aliasing.

The main problem encountered with the majority of classical downward continuation methods is that the disintegration phenomenon occurs at a much shallower depth than the true depths of shallowest sources (e.g., Fig. 1c and Fig. 1d)—due to the existence of noise and Gibb's effect on the data window edges (introduced by the discrete Fourier transformation). This is caused by the fact that the spectral characteristics of the downward continuation are those of a high pass filter and any high-frequency noise content and/or small amplitude Gibb's effects on discontinuities and edges are extremely amplified. Some authors (e.g., Ku et al., 1971) have realized that classical methods are strongly dependent upon the sampling interval of the original function and are able to downward continue only to very shallow depths – equal to a multiple of only several sampling intervals – from 2 to 10 (e.g., Xu et al., 2007). Different approaches have been published on, how to deal with this kind of instability occurring during downward continuation of potential field data (e.g., Berezkin and Buketov, 1965; Pawlowski, 1995; Fedi and Florio, 2002; Trompat et al., 2003; Cooper, 2004). In this contribution, we show the properties of the approach of Tikhonov et al. (1968), which is built upon the classical regularization concept. First trials of depth estimation by means of this regularization approach have been realized by Glasko et al. (1970). As we will show on several synthetic model studies and practical data transformation, this approach gives very stable and correct results and beside the

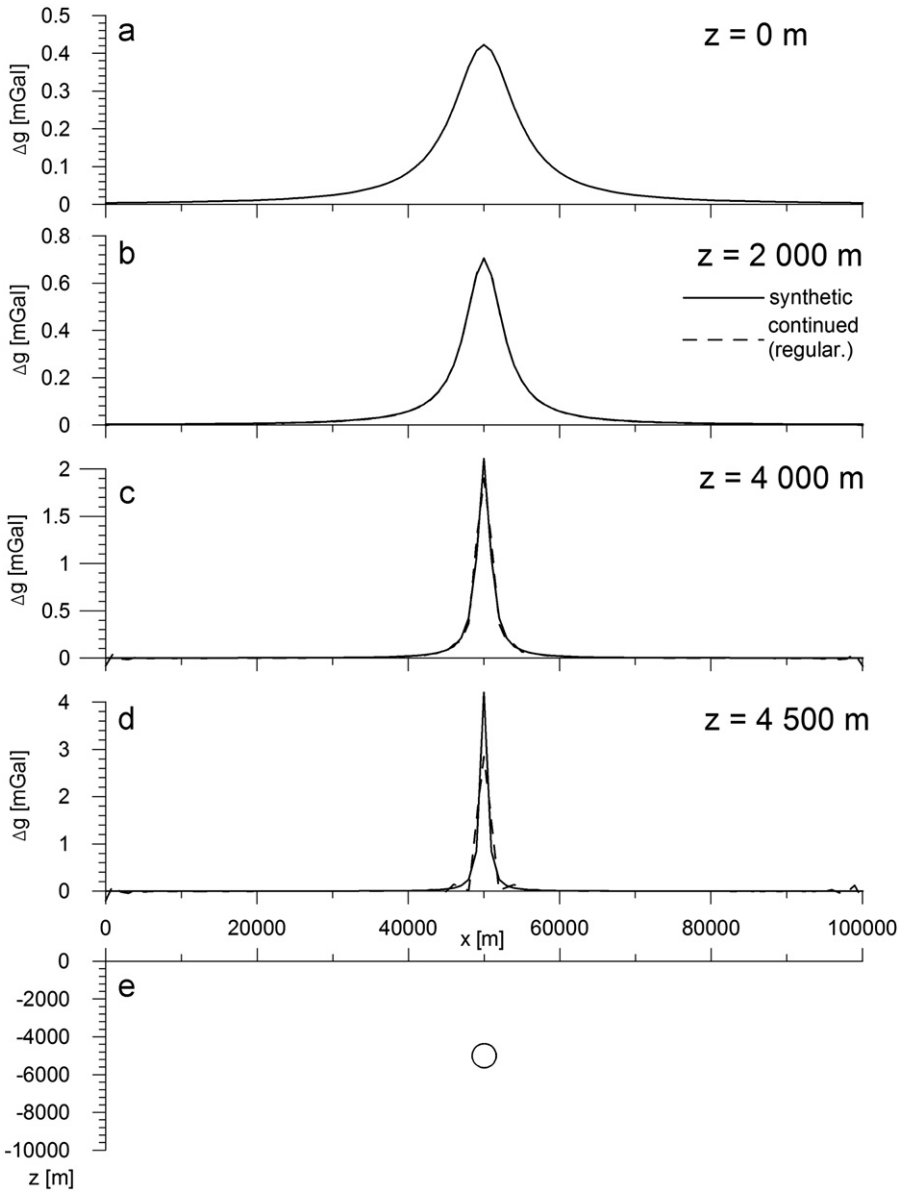

Fig. 2. Comparison of synthetic (full line) and downward continued (dashed line) gravitational field Δg by means of the *regularized approach* in spectral domain for the case of a 2D horizontal cylinder in gravimetry (a) initial depth level $z=0$ m, (b) $z=2000$ m, (c) $z=4000$ m, (d) $z=4500$ m and (e) position of the cylinder in the xz-plane; parameters of the cylinder: centre depth=5000 m, radius=500 m, differential density=200 kg m^{-3}. 1 mGal=10^{-5} m s^{-2}.

evaluation of continued field data it can be used also for the estimation of the first important source depth. In comparison with other approaches to stabilized downward continuation, it shows a relatively small dependency on the sampling rate of the data sets being interpreted.

Comment: Here we would like to point out that the presented approach is designed for the continuation of potential field data, acquired at a constant elevation level (at least with small elevation variations) or recalculated data by means of algorithms, which are able to recalculate data from an irregular surface to a horizontal plane (e.g., Cordell, 1992; Xia et al., 1993; Ivan, 1994).

2. Tikhonov regularization in downward continuation

The need for low-pass filtering of downward continued potential fields is obvious and was introduced by various authors (e.g., Berezkin and Buketov, 1965). A fascinating aspect of the Tikhonov regularization approach (Tikhonov et al., 1968; Tikhonov and Arsenin, 1977) is based on the fact that by means of a formulated minimization problem solution we can directly derive a filter form (in Fourier spectral domain) which is exactly fitted to the solved problem. For a 2D problem solution (downward continuation of a 1D function $U_0(x)$ to the depth h, $h>0$) we can write for the filter in the spectral domain the following expression (Tikhonov et al., 1968; their Eq. 27):

$$\mathbf{F}\{U_h(x)\} = \tilde{U}_h(u) = \frac{1}{1+\alpha u^2 e^{h|u|}} e^{h|u|} \tilde{U}_0(u), \tag{1}$$

where $F\{\}$ is the symbol of the direct Fourier transformation operator; $U_h(x)$ is the searched regularized downward continued function in the space domain; $\tilde{U}_h(u)$ is the Fourier transform of $U_h(x)$; $U_0(x)$ is the original function; $\tilde{U}_0(u)$ is the Fourier transform of $U_0(x)$; u is the wave-number; h is the continuation depth interval and α the so called regularization parameter (in this case a low-pass filter parameter). It is clear that the derived spectral characteristic (Eq. 1) consists of two parts: the classical for the downward continuation $\exp(h|u|)$ and a low-pass filter part

$(1/[1+\alpha u^2 \exp(h|u|)])$, where the smoothing property is given by the role of wave-number square (double integration) and exponential function (upward continuation) in the denominator and it is operated by the regularization parameter α. An optimum value of the regularization parameter α must be found individually for each processed function, which will be discussed later on. It is important to mention that the regularization approach solution produces a bias in the received solution (e.g., Cai et al., 2004), but based on our experiences with synthetic model studies it is very small in the case of the downward continuation.

We can formulate in an analogous way also the spectral characteristics of the regularized downward continuation for a 3D problem—continuation of a function $U_0^{(3D)}(x, y)$ to the depth h:

$$\mathbf{F}\left\{U_h^{(3D)}(x,y)\right\} = \tilde{U}_h^{(3D)}(u,v) = \frac{1}{1+\alpha\left(u^2+v^2\right)e^{h\sqrt{u^2+v^2}}} e^{h\sqrt{u^2+v^2}} \tilde{U}_0^{(3D)}(u,v), \tag{2}$$

where $U_h^{(3D)}(x, y)$, $\tilde{U}_h^{(3D)}(u,v)$, $U_0^{(3D)}(x, y)$ and $\tilde{U}_0^{(3D)}(u,v)$ are the corresponding equivalents of the functions used in Eq. (1); u and v are the wave-numbers in x- and y-directions, respectively. Other used symbols in Eq. (2) are identical with Eq. (1).

Correct selection of the regularization parameter α value is very important in the whole process of downward continuation–its' optimum value operates the "balance" between the classical solution

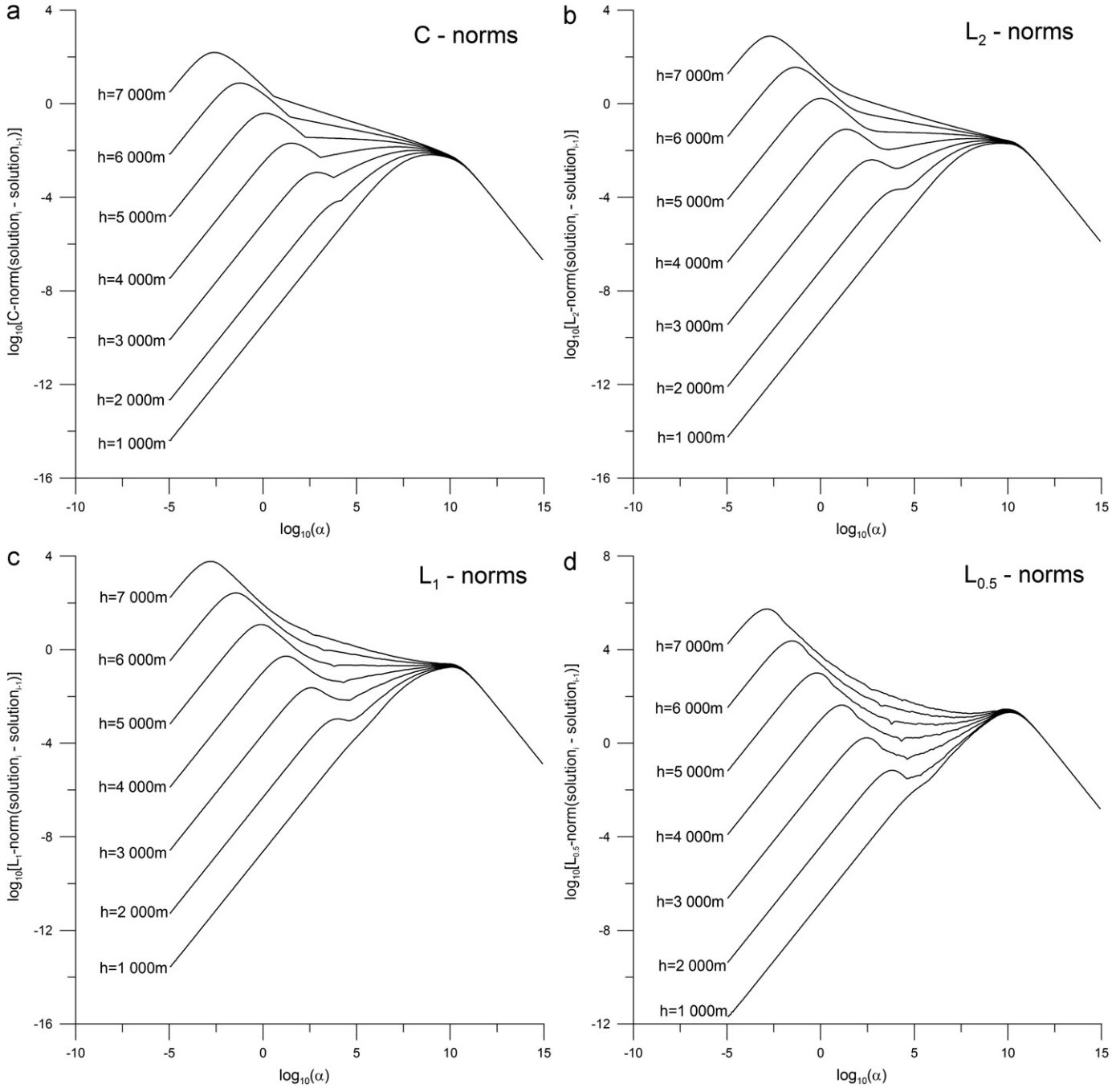

Fig. 3. Constructed L_p-norm functions for different continuation depths (from 1000 m to 7000 m) in the case of a 2D horizontal cylinder in gravimetry (displayed in Figs. 1 and 2): (a) C-norm functions, (b) L_2-norm functions, (c) L_1-norm functions and (d) $L_{0.5}$-norm functions.

(field continuation) and the low-pass aspect of the regularized solution. Estimation of the optimum value of the regularization parameter α is the crucial task and there exists a large group of different approaches (e.g., Hansen, 2007; Zhdanov, 2002; Berdichevski and Dmitriev, 2002). In the proposed algorithm we use mainly the so called *C*-norms approach (Tikhonov and Glasko, 1965; Tikhonov et al., 1968; Glasko et al., 1970; Pašteka et al., 2009), where *C*-norm (L_∞-norm) of the difference between two adjacent solutions is constructed and plotted against the used values of α (sometimes called also Chebyshev's norm). This concept is very close to the concept of *L*-curve (Lawson and Hanson, 1974; Hansen, 2007). Used values of the regularization parameter α are changed in a geometrical sequence (with the common ratio equal to 1.1), starting with very small values (e.g., 10^{-10}) and finishing with relatively large ones (e.g., 10^{+20}). The optimum value of α is usually related to a local minimum of the *C*-norm function, originated in the area between under- and over-regularized solutions (very similar to the *L*-curve), as it was theoretically argued in the work of Tikhonov and Glasko (1965)—solution should be minimally depended on the changes of the regularization parameter α. In our advanced approach we have tried to work also with other orders of the L_p-norms (L_2, L_1, $L_{0.7}$ and $L_{0.5}$). Based on the fundamental papers from Tikhonov et al. (1968) and Glasko et al. (1970), but also our empirical results we can state that in the majority of studied cases (synthetic and real world) the originally introduced *C*-norm functions analysis defines very well the position of the optimum regularization parameter value, but there are cases where other L_p-norms give better results (mainly in the case of under-sampled data sets).

To show the basic properties of the proposed approach, we show here as the first example the downward continuation of the anomalous gravitational acceleration Δg field to depths 2000 m, 4000 m and 4500 m in a case of a 2D horizontal cylinder with the centre in the depth of 5000 m (radius=500 m, differential density=200 kg m^{-3})—by means of the standard procedure without any smoothing or damping (Fig. 1) and by means of the proposed regularization approach (Fig. 2). In Fig. 1 we can clearly see the mentioned "disintegration or break-up of the field" at the depth levels, which are close to the position of the field singularity (oscillations have largest amplitudes close to the edges of the profile). In the shape of the regularized field these disturbances are greatly attenuated—oscillations have only very small amplitude (Fig. 2). On the other hand, the reconstruction of the continued anomaly in its maximum display lower values when compared with the synthetic ones (e.g., on the continuation depth of 4500 m, the maximum of the continued function reaches only approx. 67% of the synthetic anomaly). This is a "kind of a tax" for the low-passing property of the regularization approach. From the interpretational aspect it is very important to study the behaviour of evaluated norm functions during the regularization procedure (Fig. 3), mainly the *C*-norms (Fig. 3a). For very small continuation depth (1000 m) there is no local minimum, for shallow depth (2000 m) a local minimum in their shape can be seen to develop, for medium depths (3000 m and 4000 m) it is well developed (and used for optimum α estimation) and for larger ones (5000 m and more) it is no longer a minimum but remains as a deflection (the curves still shows a kind of discontinuity of 0. order—a kind of "kick-up", rather than a local minimum). Study of these local minima for different depth levels allows us to estimate a level, where such a local minimum cannot be found any more (in other words=it is not possible to find a regularized solution any more)—such a continuation level is then understood as the depth of the most important shallowest source (Tikhonov et al., 1968). In the case of the 2D horizontal cylinder model this situation occurs for the continuation depth equal to 4850 m, which is very close to the real depth of the cylinder centre of 5000 m (a relative error of 3%). We have evaluated and displayed also the L_2-, L_1- and $L_{0.5}$-norms (Fig. 3b, Fig. 3c and Fig. 3d)—to show their properties in the case of optimum α and maximum continuation depth estimation. In this case, estimated local minima for these norms give higher values of α, which leads to more smoothed solutions (for the case of the continuation depth 4500 m results are summarized in Table 1) and the definition of the local minimum cannot be performed so clearly, as in the case of the *C*-norms (Fig. 3a) (e.g., in the case of $L_{0.5}$-norm, several small local minima are developed, which make an automatic determination of the general one more complicated).

3. Algorithm description

First of all it is important to mention one important fact: this approach utilizes the FFT algorithms, so it is necessary that the input data (lines or grids) are regularly sampled. When this not

Table 1
Used optimum regularized parameter α value and corresponding relative error obtained by means of different L_p-norms utilization during the reconstruction of the Δg field (in its maximum) at the depth level 4500 m for the case of a 2D horizontal cylinder in the depth 5000 m.

Norms / parameters	*C*-norm (L_∞-norm)	L_2-norm	L_1-norm	$L_{0.5}$-norm
Optimum α [m^2]	500.8	31 79.0	12 629.4	11 357.9
Relative error [%]	67.8	61.1	55.6	56.0

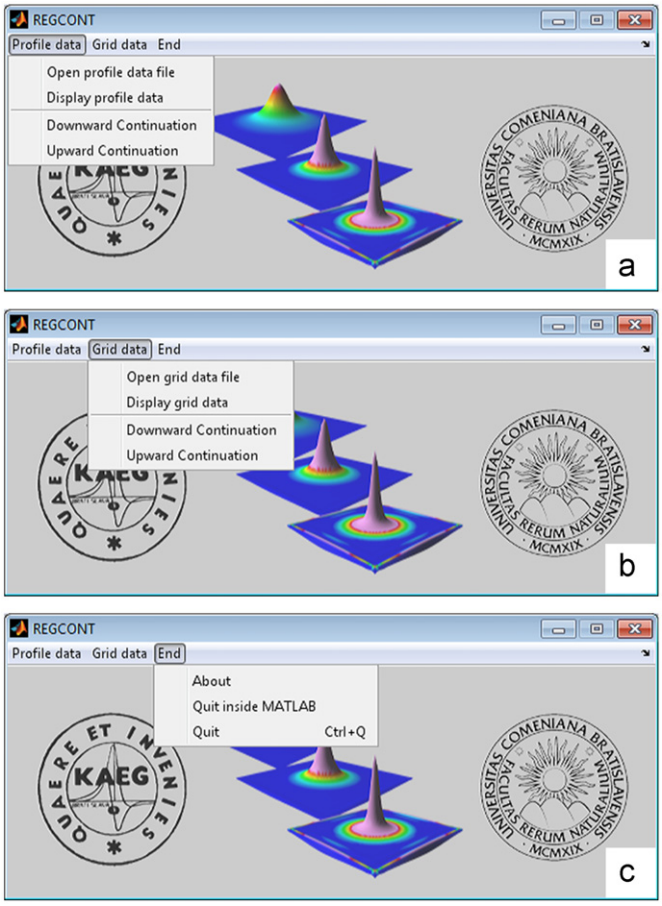

Fig. 4. Layout of the REGCONT program menus: (a) Profile data menu, (b) Grid data menu and (c) End menu.

the case, data must be firstly interpolated with a constant sampling interval by means of an appropriate method, suitable for given potential field component.

The algorithm itself is based on the following steps (we are using here functions typical for the 2D problem solution):

1. Preparation of the interpreted datasets (line data or grids) by means of an extrapolation procedure—with the aim to minimize the edge effect influence. Extrapolation is applied to profile and/or grid data sets and is realized by means of the cosine taper mirror function (Gerovska and Araúzo-Bravo, 2003; function cosxp2). Each data set is expanded by 15% of its original size in each direction (this size can be changed by the user in the code of the used function) and after realizing the transformation, final field is automatically shortened to its original size.
2. Evaluation of the Fourier transform (spectrum) $\tilde{U}_0(u)$ of the interpreted field $U_0(x)$ by means of the FFT algorithm.
3. Multiplication of the spectrum $\tilde{U}_0(u)$ by the spectral characteristics of the regularized downward continuation in the Fourier domain, given by the Eq. (1)—spectrum of the regularized solution $\tilde{U}_h(u)$ is obtained. In the low-pass filter, different values of the regularization parameter α are used—usually they are changed in a geometrical sequence.
4. Calculation of the searched regularized downward continued field in the space domain $U_h(x)$ as an inverse Fourier transform of its evaluated spectrum $\tilde{U}_h(u)$ for different values of regularization parameter α.
5. Construction of the *C*-norm function by means of the adjacent solutions (for different α) comparison: obtained solutions are subtracted each from other and the maximum absolute value of this difference is representing their distance as a *C*-norm and plotted in a graph depending of the used regularization parameter in a log–log scale (e.g., Fig. 3a). The general shape of the *C*-norm function has always a typical concave shape (convex cap shape) with a possible local minimum close to the general maximum of the function. Left-hand part of the *C*-norm function (low values of α) is displaying the difference between adjacent under-regularized and the right-hand part (high α values) between over-regularized solutions, respectively.

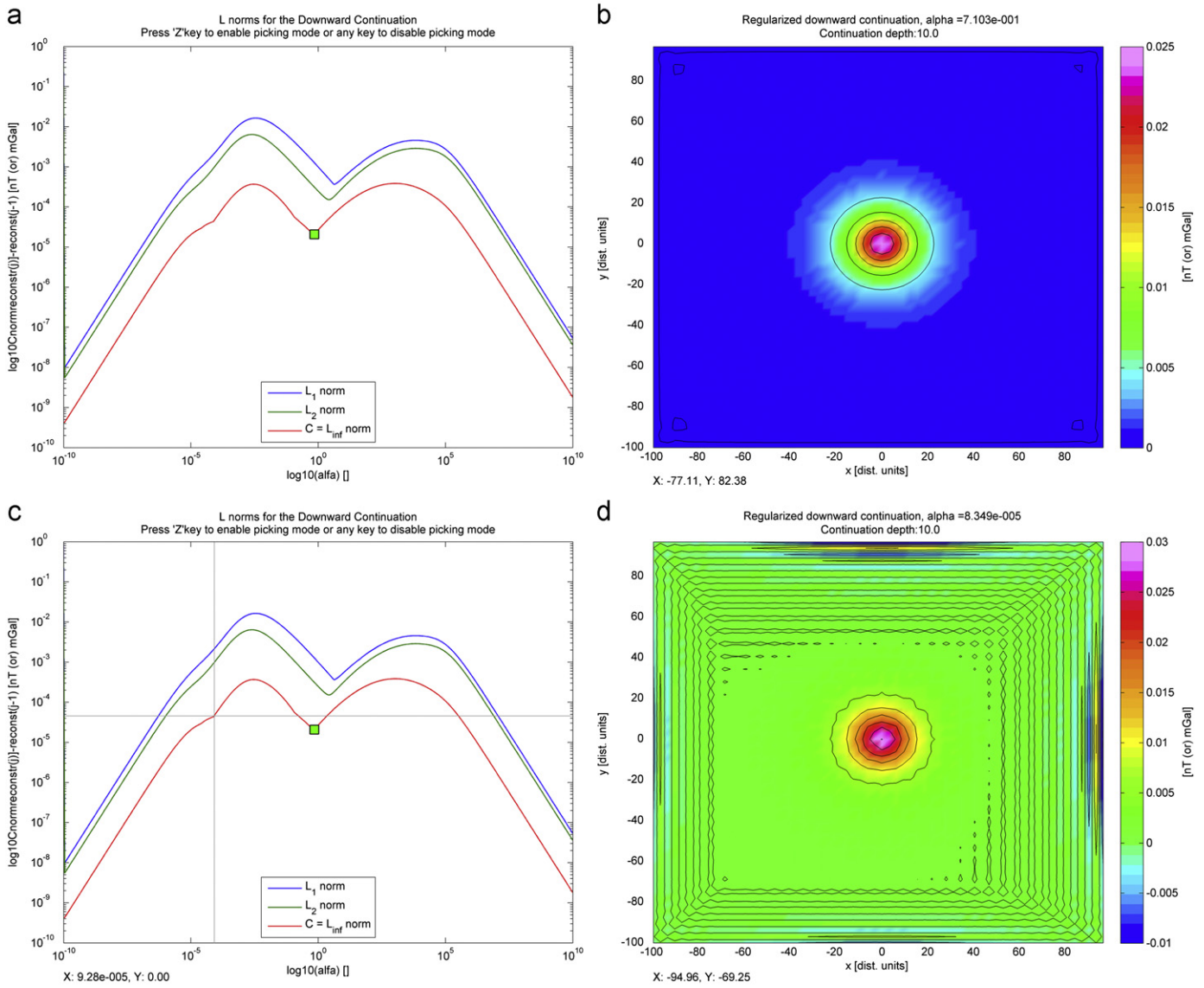

Fig. 5. Typical working windows of the REGCONT program: (a) situation with automatic detection of the local minimum in the *C*-norm function (full square), (b) corresponding evaluated regularized solution grid, (c) example of manual determination of a selected value of regularization parameter α (after clicking with the left-hand mouse button in the space of the left-hand window and pressing the *Z* button), (d) corresponding evaluated regularized solution grid.

As additional information also other L_P-norms are displayed (Fig. 3b, Fig. 3c and Fig. 3d)—for the 2D problem solution: L_2, L_1, $L_{0.7}$, $L_{0.5}$ and for the 3D problem solution: L_2, L_1.

6. Analysis of the obtained C-norm function (and/or other L_p-norm functions): as it was mentioned, optimum value of the regularization parameter α_{opt} should be connected with the developed local minimum close to the top of its concave form (e.g., Fig. 3). Position of the local minimum is detected automatically by means of a simple 3-point window (comparing the value of the central point with the side ones), starting with the C-norm function values obtained for lowest α values (left-hand begin of the C-norm function). When the used interval of α is not sufficient (the expected concave shape of the C-norm function with a local minimum close to its top is not displayed—only a part of it), one of this interval limits must be changed in a proper way (see an example given later). The user can accept the solution for the automatically detected optimum regularization parameter or try to select own optimum solution by manual changing the value of α (taking values close to the local minimum of the C-norm).
7. Finally, for the selected optimum regularization parameter α_{opt} (automatically or manually selected) the final regularized solution is calculated (again firstly in the spectral domain and then via inverse FT it is transformed into the spatial domain) and saved together with the evaluated norm functions in a form of ASCII data files.

4. Basic features of the Matlab-based program REGCONT

Program REGCONT is realized in the Matlab environment (version R2007a and higher), using basic GUI properties. Realization steps, which should be selected by the user have very a simple arrangement—sequence of data import and the transformation itself (with the selection of the optimum regularization

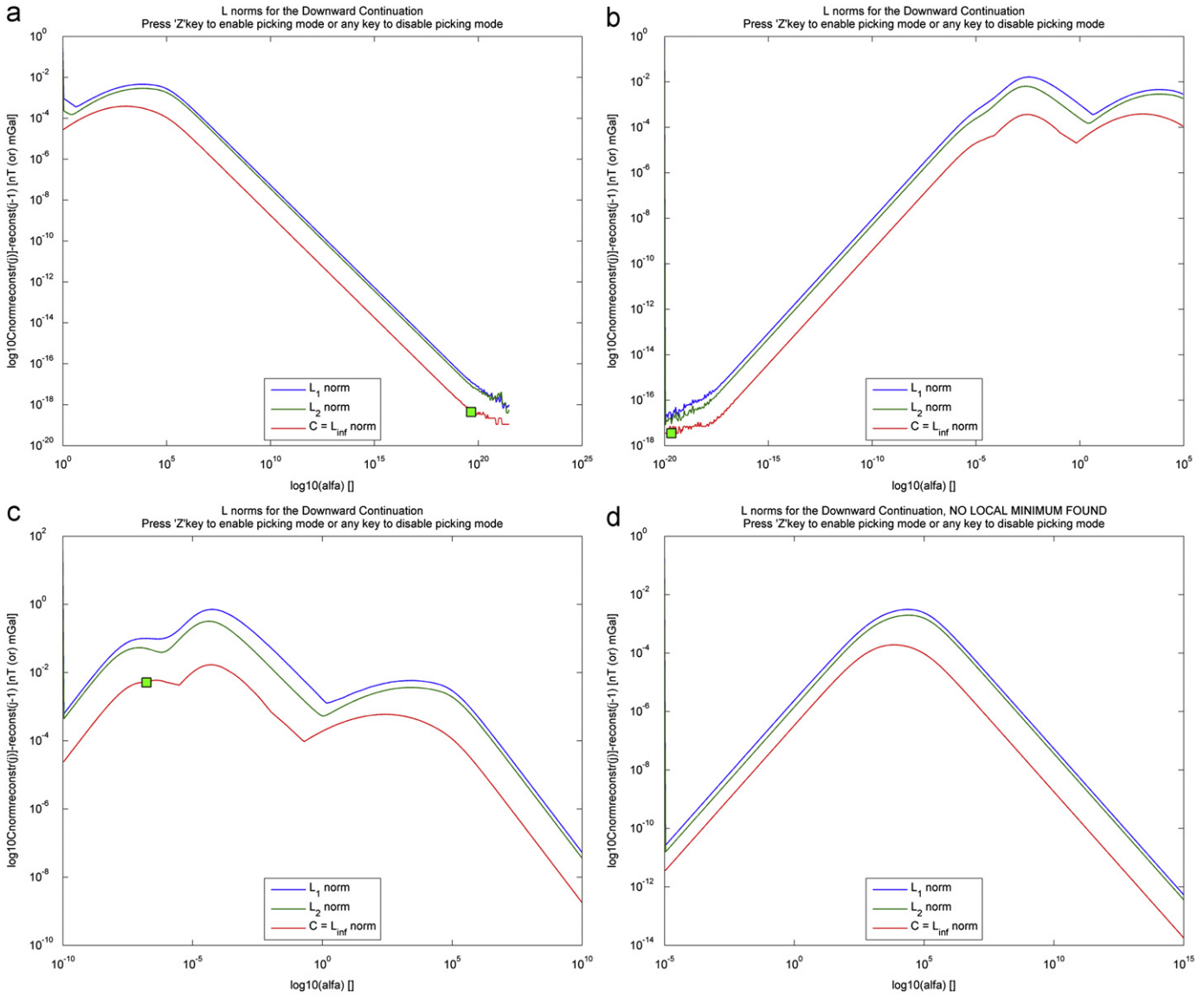

Fig. 6. Typical working windows of the REGCONT program, which show some situations connected with the norm-functions analysis: (a) wrongly (automatically) determined local minimum (full square) in the area of high α values, caused by numerical instabilities, when handling large numbers; (b) wrongly (automatically) determined local minimum (full square) in the area of low α values, caused by numerical instabilities, when handling small numbers; (c) wrongly (automatically) determined local minimum (full square), which is not the right local minimum of the C-norm function; (d) no local minimum was automatically found—in this case the reconstructed solution is a non-regularized one (for $\alpha=0$).

parameter) must be followed. The program menu is divided into three simple areas: processing of profile data, grid data and quitting the program ('Profile data', 'Grid data', 'End') (Fig. 4). In both data processing menus, firstly data import must be selected ('Open profile data file', 'Open grid data file') (Fig. 4a and Fig. 4b), data are then imported and displayed with a small information window about the size of data file (this can be immediately closed by the user). For profile data processing a simple 2 columns ASCII text file is needed (first column: x-coordinate, second column: original field); for grid data processing an ASCII Golden Software Surfer grid is expected. Imported data files can be displayed again any time—using the second item from the menus ('Display profile data', 'Display grid data') (Fig. 4a and Fig. 4b). Profile data are displayed in a form of a line graph, grid data in a form of a coloured image—using a colour scale, traditionally used in potential fields visualization, with "warm" colours (red, pink) for positive maximum values and "cold" colours (blue, green) for minimum ones.

The next step is the selection of 'Downward continuation' from the menu (Fig. 4a and Fig. 4b), where the continuation depth must be entered in a small window (it has to be in the identical distance units as they are used in the input data; plus/minus sign is not important as the program uses the absolute value of this parameter) and immediately afterwards have to be entered the start (e.g.,: 10^{-5}) and end values (e.g.,: 10^{20}) of the used regularization parameter α. After a short time of calculations two important windows are displayed (Fig. 5)—in the left-hand window the evaluated norm functions are displayed together with the automatically estimated local minimum on the C-norm function (if any) in a form of a small full square. The user now has the possibility to select manually on the graphs of norms in the left-hand window a value of regularization parameter α (after clicking with the left mouse button in the space of the left-hand window and pressing the Z key) and see the corresponding regularized solution in the right-hand window (Fig. 5). The non-regularized solution (setting $\alpha=0$) can be obtained any time by clicking the right-hand mouse button. Exiting this mode is realized by pressing an arbitrary key. Every displayed continued field is immediately saved in an output file—again in a form of a 2 columns ASCII text file for profile data and GS Surfer ASCII grid file for grid data (in the output file name the level of continuation and name of the original file are combined together with an abbreviation "DC" for downward continuation). Second output file contains the evaluated norm functions (recalculated into a

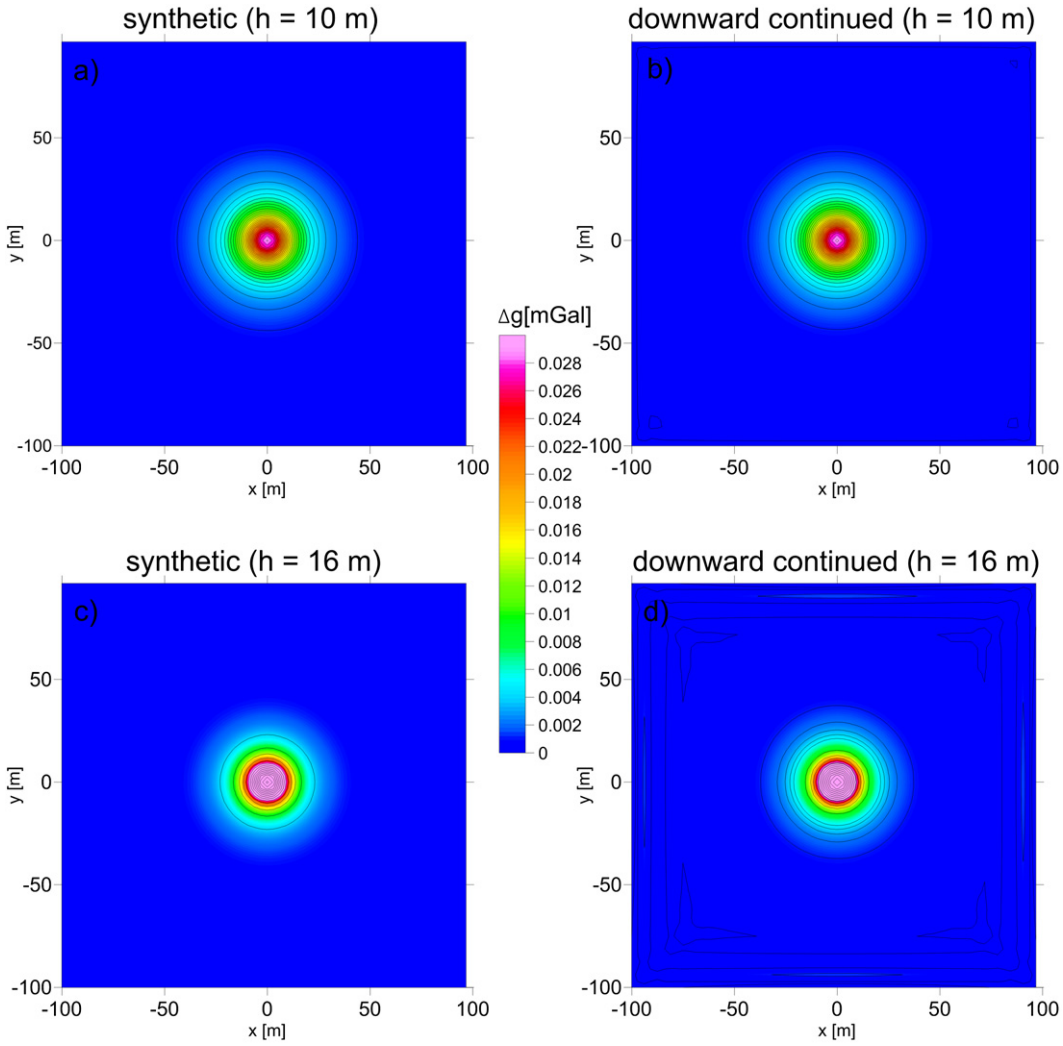

Fig. 7. Results from the downward regularized continuation of a 2D synthetic Δg field (grid) caused by a cube (dimensions: $10\times10\times10$ m; differential density: 1000 kg m^{-3}), positioned with its upper boundary in the depth 20 m; (a) synthetic Δg field at the level $h=10$ m, (b) downward regularized continued Δg field at the level $h=10$ m, (c) synthetic Δg field at the level $h=16$ m, (d) downward regularized continued Δg field at the level $h=16$ m. 1 mGal$=10^{-5}$ m s^{-2}.

common logarithm), name of this file is composed from the name of the original data file and the abbreviation "norms_DC" and again the value of the continuation depth interval.

When an insufficient interval of the regularization parameter α is selected by the user, it can happen that the local minimum of the *C*-norm function is not found and the whole process must be repeated by giving more appropriate new values for the begin and end value of α (in Fig. 6 the reader can see some examples of such situations). In the case, when no local minimum is automatically found (Fig. 6d), program is evaluating a non-regularized solution (for $\alpha=0$). Sometimes in a case of an incorrect interval of α selection it can happen that a small unimportant local minimum of the *C*-norm function from the interval begin or end is automatically found by the program (Fig. 6a and Fig. 6b)—such a minimum is not correct and user has to manually select the local minimum, which is close to the global maximum or change the interval of used α.

As an additional feature, the program contains the possibility to perform upward continuation (menu item 'Upward continuation') – in this the case the user enters the continuation depth interval in a small window (plus/minus sign is not important – the program uses the absolute value of this parameter taken with a minus sign) and the transformed field is displayed (and saved in an output file with the value of the continuation depth interval and abbreviation "UC" in its name).

5. Synthetic and real-data examples of regularized downward continuation

To show the properties of the proposed method for stable downward continuation we have selected four synthetic models and one practical case, coming from a test measurement over an ammunition projectile recorded at two elevation levels (obtained in a frame of a local project of UXO detection; UXO=UneXploded Ordnance).

Next synthetic example (the first one was given in the section describing the regularization approach) represents the downward continuation of a 2D Δg field (grid) caused by a cube (dimensions: $10\times10\times10$ m; differential density: 1000 kg m^{-3}), positioned with its upper boundary in the depth 20 m. In Fig. 7 there are selected two typical results for the continuation levels $h=10$ m and $h=16$ m (synthetically derived field at the same depth level as the downward continued regularized field). Qualitative comparison with synthetic data shows a very good ability of the regularization algorithm to give reliable results also on levels close to the source position (a weak edge effect still occur, Fig. 7b and Fig. 7d). From the analysis of the evaluated *C*-norms functions (Fig. 8) it follows that the vanishing of the local minimum in the *C*-norm functions occurs at the depth 25 m, which corresponds exactly to the centre of the cube. From the point of view of continued data reconstruction we must be always very careful—for larger depths (close to the main singularity), the continued field does not represent the real field (which could be measured on this level), but a kind of transformed low-pass filtered (deformed) field. Similar transformed downward continued fields are utilized also in the normalized full gradient method (Berezkin, 1988; Elysseieva, 1995; Elysseieva and Pasteka, 2009), where the transformation into the source region is realized only in a formal way (also deeper then the important shallower sources) to obtain information about the sources depths.

Next two synthetic model studies results (focused on the source depth estimation) are summarized in Tables 2 and 3. In this case 2D magnetized bodies (horizontal cylinder with radius=2 m and vertically limited thin sheet with thickness=2 m) have been positioned in the centre of a 500 m long profile and the modelled ΔT field was sampled with different steps ($\Delta x=1$, 5 and 10 m) (parameters of the induced magnetization: susceptibility=0.05 SI units, inducing field induction=48,000 nT, its inclination=65° and declination=0°). The majority of the estimations has been realized by means of the *C*-norm function analysis (not shown here), but in the case of undersampled data sets ($\Delta x=5$ and/or 10 m) there could not be detected a local minimum in the *C*-norm shapes—other L_p-norms have shown better properties (mainly the $L_{0.5}$-norm). From the results

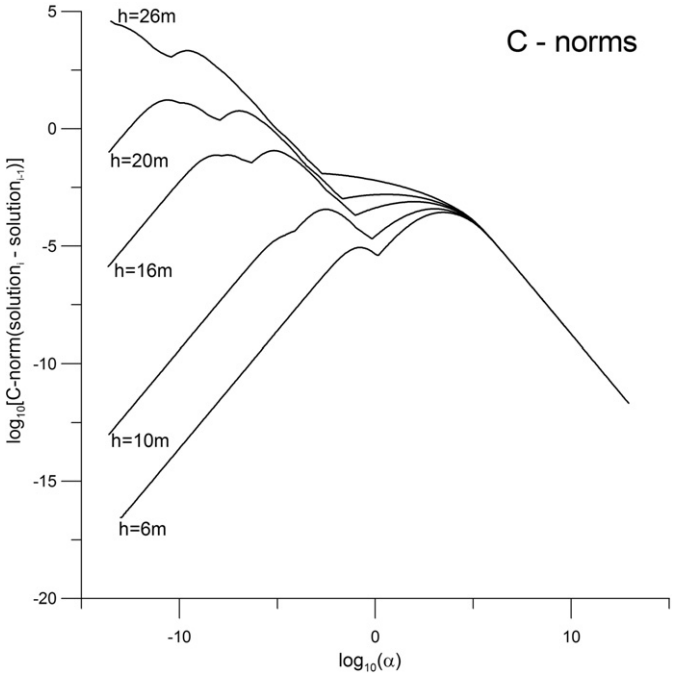

Fig. 8. Constructed *C*-norm functions for different continuation depths (from 6 m to 26 m) in the case of a 2D synthetic Δg field (grid) caused by a cube in gravimetry (displayed in Fig. 7).

Table 2
Source depth estimation by means of regularized downward continuation and norm function analysis in the case of a 2D magnetized horizontal cylinder with radius of 2 m (h=centre depth) for various used sampling steps $\Delta x=1$, 5 and 10 m; profile length=500 m. (C) – depth estimation has been realized by means of *C*-norm function analysis, ($L_{0.5}$) – depth estimation has been realized by means of $L_{0.5}$-norm function analysis.

Centre depth / sampl. step [m]	$h=2$ m	$h=5$ m	$h=10$ m	$h=20$ m	$h=50$ m
1	1.8 (*C*)	5.1 (*C*)	9.8 (*C*)	18.3 (*C*)	41.6 (*C*)
5	6.0 ($L_{0.5}$)	6.0 ($L_{0.5}$)	8.8 (*C*)	19.6 (*C*)	41.4 (*C*)
10	15.0 ($L_{0.5}$)	9.5 ($L_{0.5}$)	11.0 ($L_{0.5}$)	17.6 (*C*)	49.3 (*C*)

Table 3
Source depth estimation by means of regularized downward continuation and norm function analysis in the case of a 2D magnetized vertically limited thin sheet with the thickness of 2 m (h_1 and h_2=upper and bottom edge depths) for various used sampling steps $\Delta x=1$, 5 and 10 m; profile length=500 m. (C) – depth estimation has been realized by means of *C*-norm function analysis, ($L_{0.5}$) – depth estimation has been realized by means of $L_{0.5}$-norm function analysis.

Vert. extent / sampl. step [m]	$h_1=10$ m $h_2=12$ m	$h_1=10$ m $h_2=20$ m	$h_1=10$ m $h_2=50$ m	$h_1=10$ m $h_2=100$ m
1	10.0 (*C*)	10.1 (*C*)	10.0 (*C*)	10.0 (*C*)
5	9.9 (*C*)	12.2 (*C*)	13.1 (*C*)	13.1 (*C*)
10	11.7 ($L_{0.5}$)	11.9 ($L_{0.5}$)	13.6 ($L_{0.5}$)	16.0 ($L_{0.5}$)

(Tables 2 and 3) we can see that in the case of the cylinder its centre is recognized as the most important source of the structure and for the vertical sheet it is its upper edge. For both studied bodies estimations have been wrong (too deep) in the case of under-sampled data sets (when the source depth was smaller than the size of the sampling step). In the case of the horizontal cylinder for short profile lengths estimations have been too shallow (when the source depth was larger than the tenth of the profile length). For well sampled data sets ($\Delta x = 1$ m) and an appropriate profile length, the estimates gave satisfactory results in both cases.

As a practical data set for processing and interpretation, we have selected high-definition magnetometry data set (acquired by a Cs-vapour magnetometer model TM-4), obtained from test measurements over an UXO object (projectile with 100 mm diameter, lying on the surface and pointing with its elongated shape into the direction of the inducing Earth magnetic field vector direction)—acquired in two elevations: in the level of 0.7 m and 1 m over the ground (Fig. 9), during a project focused on the analysis of the magnetic properties of UXO objects. Data were acquired along profiles 1 m apart from each other with 0.1 m sampling step, processed in a standard way into the form of ΔT field and than interpolated into a 0.1×0.1 m grid by means of the kriging method (GS Surfer 8 software). The acquired ΔT field at the elevation level 1 m over the ground (Fig. 9b) was then downward continued by means of the proposed regularization approach (selecting the optimum regularization parameter from the local minimum of constructed C-norm function) to the level 0.7 m over the ground (Fig. 9c) and compared with the measured values at this level (Fig. 9a). The difference between the continued and measured field (Fig. 9d) reaches relatively high amplitudes (range: from -68.1 to 29.6 nT) in comparison with the measured field (range: from -124.9 to 188.1 nT), but the main qualitative character of the continued field fits quite well with the measured one (visible on selected typical profile with constant $x = 105$ m, Fig. 10). Analysis of the C-norm functions during the downward continuation to greater depths (with the aim to estimate the depth of the source) did not offered a satisfying result (Fig. 11a)—the occurrence of the local minimum vanished shortly after passing the depth level 0.6 m. A better result (but still erroneous) was obtained by the analysis of L_1-norm functions (Fig. 11b)—the source depth was estimated at the depth 0.75 m, which means a relative error of 21.1% in comparison with the real depth of the projectile (0.95 m). This error is relatively large, but still usable in the comparison with other depth-estimation methods, traditionally used in potential fields' interpretation. Better result, obtained by means of the use of L_1-norms, was probably obtained due to the situation with under-sampled data sets (as it was shown in the case of the magnetized cylinder and vertical thin sheet, summarized in Tables 2 and 3).

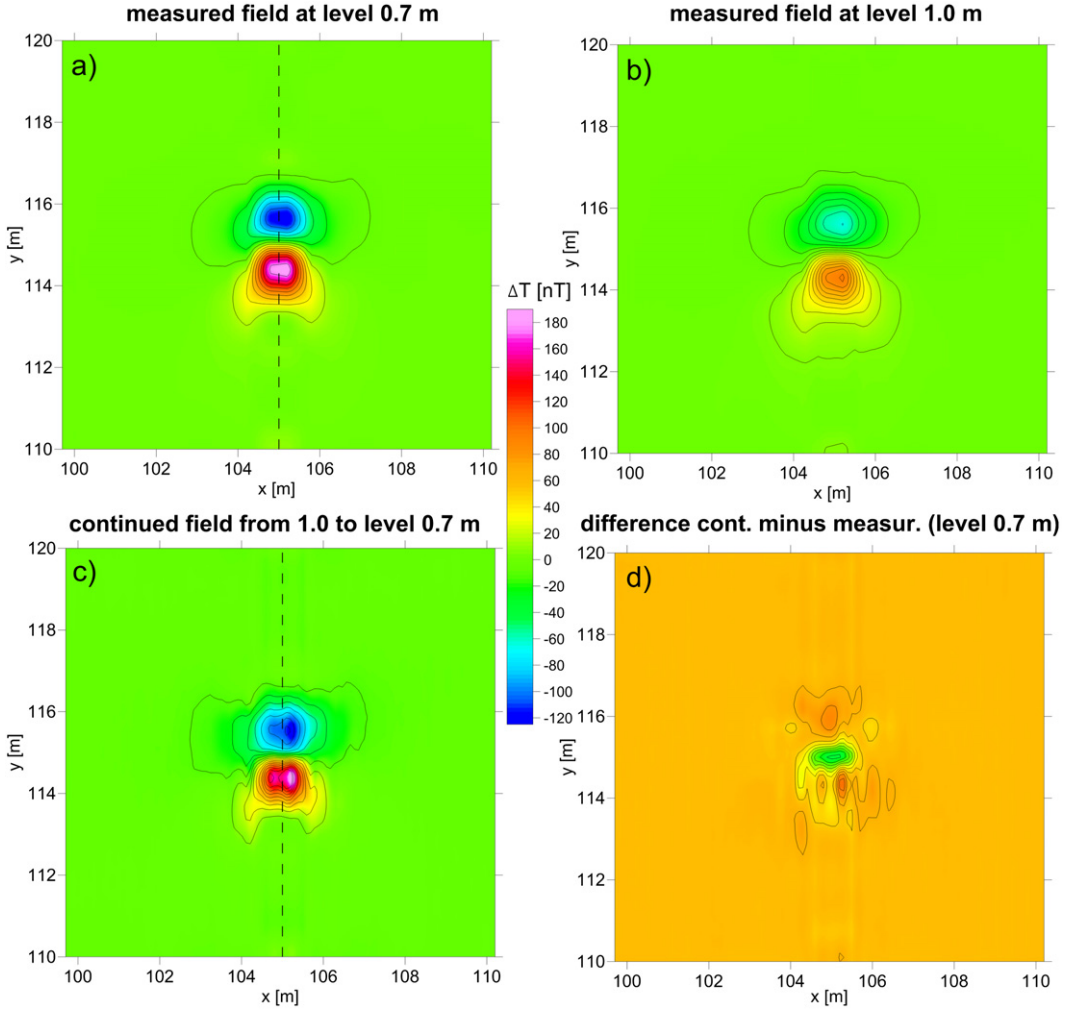

Fig. 9. High-definition magnetometry data set (ΔT field), acquired over an 100 mm diameter UXO object, lying on the surface in two elevations: in the level of 0.7 m and 1 m over the ground together with results of the regularized downward continuation: (a) measured ΔT field at the elevation 0.7 m over the ground; (b) measured ΔT field at the elevation 1.0 m over the ground; (c) downward continued field from the level 1.0 m to 0.7 m; (d) difference: continued minus acquired ΔT field. Dashed line in (a) and (c) is the position of a visualization profile at $x = 105$ m (values are displayed in Fig. 10).

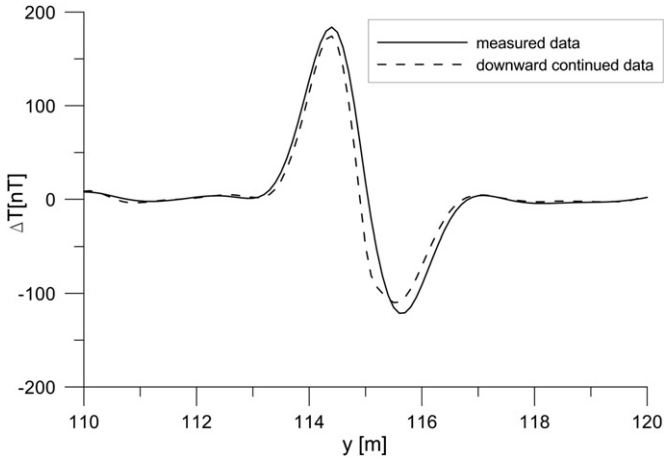

Fig. 10. Comparison of downward continued and acquired ΔT field at the level 0.7 m for the high-definition UXO magnetometry example: values along a profile with constant $x=105$ m are displayed (solid line—measured data; dashed line—downward continued).

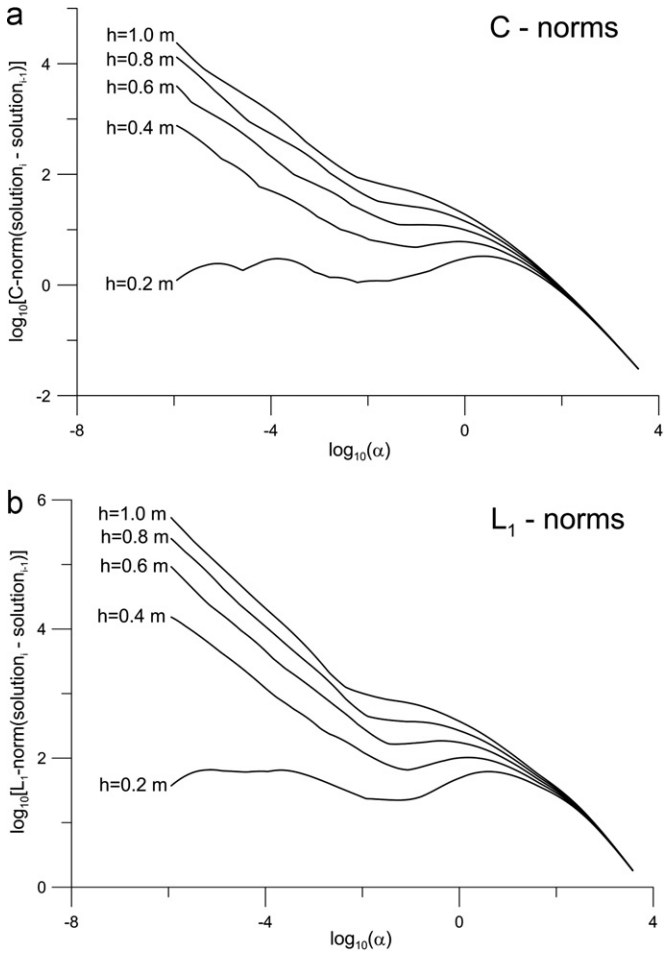

Fig. 11. Constructed C-norm and L_1-norm functions for different continuation depths (from 0.2 m to 1.0 m) (example in Figs. 9 and 10): (a) C-norm functions and (b) L_1-norm functions.

6. Conclusions

Regularization approach (Tikhonov et al., 1968) gives a straight-forward and elegant way to the solution of the problem of achieving stable downward continuation of potential fields—a low-pass filter in the Fourier spectral domain that can be derived from the solution of a clearly defined minimization problem. As we have shown on presented synthetic model studies and practical data transformation, the proposed regularization method gives stable results, which are relatively close to the correct values (particularly at shallow continuation depths). In comparison with other approaches to stabilized downward continuation, it shows a relative small dependency on the sampling rate of the data sets to be interpreted (it is not working well with strongly under-sampled data sets, where the source depth is smaller than the size of the sampling step). Beside the evaluation of the continued field data it can be used also for the estimation of the depth to the most important shallowest source—in the case of structures with an isometric cross-section it is the centre, for thin vertically extended bodies its upper edge.

For the selection of the optimum regularization parameter value α, the behaviour of the constructed norm functions has been used. In the majority of cases, C-norms gave a better developed and necessary local minimum in the function shape, which is connected with the searched optimum α value. Positions of local minima for other L_p-norm functions give in general higher values of α, which leads to more smoothed solutions. On the other hand, in some cases these norm functions can give a better developed local minimum and so they can be used better for depth estimation purposes (mainly in the case of under-sampled data sets). We plan to study this aspect in more details in the future, now from our achieved experience we always try to analyse that kind of norm functions, which give us the best developed and clearly defined local minima over shallower depths analysis and look after the (greater) depth, when this minimum vanishes.

Acknowledgements

Authors would like to thanks for a long-term mental and technical support in the area of regularization methodology from P.F. Richter, K. Brazda, B. Meurers, J. Brestenský and H.-J. Götze. We are also thankful to J. Mikuška from G-trend Ltd. for the permission to use the UXO high-definition magnetometry data and to John Stanley for the great help the improvement of the original manuscript. The scientific work on this topic was realized in the frame of projects VEGA 1/0095/12, 2/0067/12, 1/0747/11, APVV-0724-11 and mainly APVV-0194-10.

Appendix A. Supporting information

Supplementary data associated with this article can be found in the online version at http://dx.doi.org/10.1016/j.cageo.2012.06.010.

References

Baranov, W., 1975. Potential Fields and their Transformations in Applied Geophysics. Gebrüder Borntraeger, Berlin Stuttgart 151 pp.

Berdichevski, M.N., Dmitriev, V.I., 2002. Magnetollurics in the Context of the Theory of ILL-Posed Problems. Society of Exploration Geophysicists, Tulsa 230 pp.

Berezkin, V.M., 1988. Method of the Total Gradient in Geophysical Prospecting. Nedra, Moscow 189 pp. [in Russian].

Berezkin, V.M., Buketov, A.P., 1965. Application of the harmonic analysis for the interpretation of gravity data. Prikladnaya Geofizika (Applied Geophysics) 46, 161–166. [in Russian].

Bullard, E.C., Cooper, R.I., 1948. Determination of masses necessary to produce a given gravitational field. Proceedings of the Royal Society A 194, 332–347.

Cai, J., Grafarend, E.W., Schaffrin, B., 2004. The A-optimal regularization parameter in uniform Tykhonov-Phillips regularization: alpha weighted BLE. in: Sansó, F. (Ed.), 5th Hotine—Marussi Symposium on Math. Geodesy, IAG Symposia, Vol. 127. Springer Verlag, Berlin-Heidelberg, pp. 309–324.

Cooper, G., 2004. The stable downward continuation of potential field data. Exploration Geophysics 35, 260–265.

Cordell, L., 1992. A scattered equivalent-source method for interpolation and gridding of potential-field data in three dimensions. Geophysics 57, 629–636.
Elysseieva, I.S., 1995. Methodical Recommendations for the Interpretation of Gravity and Magnetic Data by Means of the Quasisingular Points Method. VNIIGeofizika, Geoinfomark, Moscow. [in Russian].
Elysseieva, I.S., Pasteka, R., 2009. Direct interpretation of 2D potential fields for deep structures by means of the quasi-singular points method. Geophysical Prospecting 57, 683–705.
Evjen, H.M., 1936. The place of the vertical gradient in gravitational interpretations. Geophysics 1, 127–136.
Fedi, M., Florio, G., 2002. A stable downward continuation by using the ISVD method. Geophysical Journal International 151, 146–156.
Fedi, M., Florio, G., 2011. Normalized downward continuation of potential fields within the quasi-harmonic region. Geophysical Prospecting 59, 1087–1100.
Gerovska, D., Araúzo-Bravo, M.J., 2003. Automatic interpretation of magnetic data based on Euler deconvolution with unprescribed structural index. Computers & Geosciences 29, 949–960.
Glasko, V.B., Litvinenko, O.K., Melikhov, V.R., 1970. Possibilities of regularizing algorithms for continuation of potential functions close to source masses. Prikladnaya Geofizika (Applied Geophysics) 60, 142–157. [in Russian].
Hansen, P.C., 2007. Regularization tools version 4.0 for Matlab 7.3. Numerical Algorithms 46, 189–194.
Hughes, D.S., 1942. The analytic basis for gravity interpretation. Geophysics 7, 169–178.
Ivan, M., 1994. Upward continuation of potential fields from a polyhedral surface. Geophysical Prospecting 42, 391–404.
Jung, K., 1961. Schwerkraftverfahren in der angewandten Geophysik. AV Geest & Portig, Leipzig, 348 pp. in German.
Ku, C., Telford, W., Lim, S., 1971. The use of linear filtering in gravity problems. Geophysics 36, 1174–1203.
Lawson, C.L., Hanson, R.J., 1974. Solving Least Squares Problems. Prentice-Hall, Englewood Cliffs 305 pp.
Mudretsova, E.A., Veselov, K.A. (Eds.), 1990. Nedra, Moscow 607 pp. [in Russian].
Nabighian, M.N., 1974. Additional comments on the analytic signal of two dimensional magnetic bodies with polygonal cross-section. Geophysics 39, 85–92.
Parker, R.L., 1977. Understanding Inverse Theory. Annual Review of Earth and Planetary Sciences 5, 35–64.
Pašteka, R., Richter, F.P., Karcol, R., Brazda, K., Hajach, M., 2009. Regularized derivatives of potential fields and their role in semi-automated interpretation methods. Geophysical Prospecting 57 (4), 507–516.
Pawlowski, R.S., 1995. Preferential continuation for potential-field anomaly enhancement. Geophysics 60, 390–398.
Peters, L.J., 1949. The direct approach to magnetic interpretation and its practical application. Geophysics 14, 290–320.
Roy, K.K., 2008. Potential Theory in Applied Geophysics. Springer-Verlag, Berlin, Heidelberg 651 pp.
Tikhonov, A.N., Glasko, V.B., 1965. Application of the regularization method to nonlinear problems. Zh. vychislit. matem. i matem. fiz., 5, N 3, 463–473. [in Russian].
Tikhonov, A.N., Glasko, V.B., Litvinenko, O.K., Melikhov, V.R., 1968. Analytic continuation of a potential in the direction of disturbing masses by the regularization method. Izv., Earth Physics 12, 30–48. [in Russian; English translation: 738–747].
Tikhonov, A.N., Arsenin, B.J., 1977. Solutions of ILL-Posed Problems. John Wiley& Sons, New York.
Trompat, H., Boschetti, F., Hornby, P., 2003. Improved downward continuation of potential field data. Exploration Geophysics 34 (4), 249–256.
Tsuboi, C., Fuchida, T., 1937. Relations between the gravity values and corresponding subterranean mass distribution. Earth Research Institute of Tokyo Imperial University Bulletin 15, 639–649.
Xia, J., Sprowl, D.R., Adkins-Heljeson, D., 1993. Correction of topographic distortions in potential-field data: a fast and accurate approach. Geophysics 58, 515–523.
Xu, S., Yang, J., Yang, C., Xiao, P., Chen, S., Guo, Z., 2007. The iteration method for downward continuation of a potential field from a horizontal plane. Geophysical Prospecting 55, 883–889.
Zhdanov, M.S., 2002. Geophysical Inverse Theory and Regularization Problems. Elsevier 609 pp.